Kinetic model for electron-ion transport in warm dense matter

Shane Rightley [*]
Department of Physics and Astronomy, University of Iowa, Iowa City, Iowa 52242, USA

Scott D. Baalrud [†]
Department of Nuclear Engineering and Radiological Sciences, University of Michigan, Ann Arbor, Michigan 48109, USA

(Received 9 February 2021; revised 3 May 2021; accepted 3 May 2021; published 14 June 2021)

We present a model for electron-ion transport in warm dense matter that incorporates Coulomb coupling effects into the quantum Boltzmann equation of Uehling and Uhlenbeck through the use of a statistical potential of mean force. Although the model presented here can be derived rigorously in the classical limit [S. D. Baalrud and J. Daligault, Phys. Plasmas **26**, 082106 (2019)], its quantum generalization is complicated by the uncertainty principle. Here we apply an existing model for the potential of mean force based on the quantum Ornstein-Zernike equation coupled with an average-atom model [C. E. Starrett, High Energy Density Phys. **25**, 8 (2017)]. This potential contains correlations due to both Coulomb coupling and exchange, and the collision kernel of the kinetic theory enforces Pauli blocking while allowing for electron diffraction and large-angle collisions. We use the Uehling-Uhlenbeck equation to predict the momentum and temperature relaxation times and electrical conductivity of solid density aluminum plasma based on electron-ion collisions. We present results for density and temperature conditions that span the transition from classical weakly-coupled plasma to degenerate moderately-coupled plasma. Our findings agree well with recent quantum molecular dynamics simulations.

DOI: 10.1103/PhysRevE.103.063206

I. INTRODUCTION

The microscopic physics of warm dense matter (WDM) is subject to a multitude of physical effects, including electron degeneracy, partial ionization, large-angle scattering, diffraction, and moderate Coulomb coupling leading to correlations. Such conditions are present in experiments involving extreme compression of materials [1–3], in astrophysics [4,5], and along the compression path in inertial confinement fusion (ICF) experiments [6]. As a result of the demanding conditions for theoretical modeling, the description of WDM has been highly reliant on computational techniques. However, *ab initio* computation proves too expensive for many problems, whereas faster methods often involve uncontrolled approximations or have uncertain applicability. To support computational efforts, explore larger regions of parameter space, and expediently provide data tables for hydrodynamic simulations, reliable and fast tools for the computation of transport coefficients in WDM remain desirable.

In this work, we introduce a model for electron-ion transport based on the quantum Boltzmann equation of Uehling-Uhlenbeck [7], but with a modification motivated by the classical mean force kinetic theory [8] in which aspects of many-body interactions are modeled by treating binary collisions as occurring via the potential of mean force (PMF). The model accounts for at least some degree of partial ionization, electron degeneracy, moderate Coulomb coupling, diffraction, and large-angle collisions. The approximate regimes in which these different physical processes are important can be roughly understood in terms of the degeneracy parameter $\Theta \equiv T_e/T_F$ and Coulomb coupling parameter $\Gamma = \langle U \rangle / \langle K \rangle$ with the statistical averages taken using a Maxwell-Boltzmann distribution for ions and a Fermi-Dirac distribution for electrons. T_e is the electron temperature, $T_F \equiv E_F/k_B$ the Fermi temperature, $\langle U \rangle$ the average interaction energy and $\langle K \rangle$ the average kinetic energy of a particle. The average speed of electrons shifts from the thermal speed to the Fermi speed as degeneracy increases, a phenomenon that causes electrons to become increasingly weakly coupled at high density. The Coulomb couplings Γ_{ii} and Γ_{ie} for ion-ion and electron-ion interactions, respectively, can be expressed as

$$\Gamma_{ii} = \frac{Z^2 e^2/a}{k_B T} \tag{1}$$

and

$$\Gamma_{ie} = \frac{Ze^2/a}{k_B T} \frac{\mathrm{Li}_{3/2}[-\xi]}{\mathrm{Li}_{5/2}[-\xi]}, \tag{2}$$

where $a = (3/4\pi n)^{1/3}$ is the Wigner-Seitz radius, Li is the polylogarithm function (closely related to the Fermi integral) and $\xi \equiv \exp(\mu/k_B T)$ where μ is the electron chemical potential related to Θ through the normalization of the Fermi-Dirac distribution [9]:

$$-\mathrm{Li}_{3/2}[-\xi] = \frac{4}{3\sqrt{\pi}} \Theta^{-3/2}. \tag{3}$$

[*] shane-rightley@uiowa.edu
[†] baalrud@umich.edu

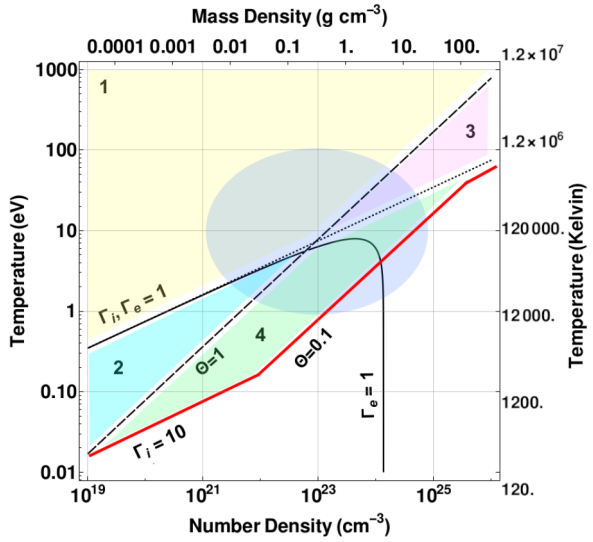

FIG. 1. Parameter regimes of fully ionized hydrogen plasma. The solid black line is the boundary between weak and strong electron coupling $\Gamma_e = 1$ and turns over due to the electron degeneracy; the dotted lined is the separation between weak and strong ion coupling $\Gamma_i = 1$; and the dashed line is the separation between classical and degenerate electrons $\Theta = 1$. The darker blue oval denotes the sector of WDM. Region 1 (yellow) is classical weakly coupled plasma; region 2 (light blue) is characterized by classical strong coupling; region 3 (pink) by quantum weak coupling; and region 4 (green) by both quantum electrons and strongly coupled ions. We expect the theory presented here to apply to each region 1–4. The red line demarcates the region of validity of plasma-type transport theories; beyond this is the regime of condensed matter.

The conditions $\Gamma = 1$ and $\Theta = 1$ divide the density-temperature parameter space into multiple regions, as seen in Fig. 1. The regimes can be broken down into (1) classical weakly coupled, (2) classical strongly coupled, (3) quantum weakly coupled, and (4) classical strongly coupled ions with degenerate weak or strongly coupled electrons. WDM exists at the intersection of all of these regions marked by the blue oval, where no small expansion parameter is available. Transport in region (1) is well-understood in terms of the Landau-Spitzer theory [10], and region (3) has been successfully modeled through quantum weak-coupling theories such as the quantum Landau-Fokker-Planck equation [11]. Progress has recently been made extending classical plasma transport theory into region (2) for $\Gamma \lesssim 20$ through use of mean force kinetic theory (MFKT) [8,12,13], which has also been successfully applied in region (4) for WDM in the case of ion transport [14]. Other existing kinetic methods for predicting transport in WDM typically fall into the categories of binary collision theories [11,15–18], linear response theories [19–21], and nonequilibrium Green's functions and field-theoretic methods [22–25].

The model presented in this work is physically intuitive, contains much of the relevant physics, and can be evaluated relatively quickly. It is based on the Uehling-Uhlenbeck equation (named BUU equation from this point on, with the letter B referencing Boltzmann), which accounts for degeneracy and diffraction [7]. Correlations in a moderate Coulomb coupling regime are modeled through the assertion that the binary scattering is mediated by the equilibrium statistical potential of mean force (PMF). The PMF is computed using a recent combined Average-Atom + Two-Component-Plasma model [18,26]. The result has the advantage of retaining the dominant aspects of the relevant physics, while remaining relatively fast to evaluate in comparison to fully dynamical calculations. In the classical limit the model can be rigorously derived [8], but while this derivation cannot be easily extended to the quantum domain due to the uncertainty principle, it is reasonable to apply the PMF to the BUU equation.

Explicit results are computed for momentum and energy relaxation rates of aluminum at conditions spanning the WDM regime. The results for energy relaxation are found to be equivalent to a recent model by Daligault and Simoni [27] if interactions are assumed to occur via the PMF in that theory. It is found that large-angle collisions contribute to the momentum relaxation rate and thus the electrical conductivity. Predictions made with our theory show good agreement with quantum molecular dynamics simulations of electrical conductivity at WDM conditions [28].

We begin by detailing the model in Sec. II. We introduce the PMF into the BUU equation and discuss what the concept means in the context of a degenerate plasma. In Sec. III we apply this to electron-ion momentum and temperature relaxation, where we obtain the degeneracy- and correlation-dependent "Coulomb integral" that replaces the traditional Coulomb logarithm. In Sec. IV, we evaluate the model for the solid-density aluminum and compare to common and simple alternatives and discuss the relative importance of the effects of correlation, large-angle scattering, Pauli blocking, and diffraction. We conclude and summarize in Sec. V.

II. A KINETIC EQUATION FOR TRANSPORT IN WDM

A. The Uehling-Uhlenbeck collision operator

We consider the collision integral from the right-hand side of the BUU equation [7],

$$C_q^{ss'} = \int d\boldsymbol{v}' d\Omega \frac{d\sigma}{d\Omega} u[\hat{f}_s \hat{f}_{s'}(1+\theta_s f_s)(1+\theta_{s'} f_{s'}) - f_s f_{s'}(1+\theta_s \hat{f}_s)(1+\theta_s \hat{f}_{s'})], \quad (4)$$

where $\boldsymbol{u} \equiv \boldsymbol{v} - \boldsymbol{v}'$ is the relative velocity of the scattering particles, the "hatted" quantities $\hat{f}_s$ are evaluated at the post-collision velocity $\hat{\boldsymbol{v}} = \boldsymbol{v} + \Delta\boldsymbol{v}$ and $\theta_s = (\pm 1/g_s)(h/m_s)^3$ where g_s is an integer accounting for particle statistics with $g_s = g_e = 2$ for electrons, the + sign corresponds with Bosons and the − sign with Fermions. Calculation of $d\sigma/d\Omega$ is carried out via a partial wave expansion in terms of the phase shifts $\delta_l(\eta)$. The determination of the phase shifts from the Schrödinger equation is discussed in the Appendix.

The BUU equation describes the evolution of the Wigner quasi-probability distribution function f_s. It was originally proposed as an extension of the Boltzmann equation to account for degeneracy [7], but a consistent derivation of the equation was not accomplished for some time. Early methods involved applying the BBGKY hierarchy to the kinetic

equation for the Wigner function and often fell short of fully obtaining the BUU equation, i.e., to include the θ_s terms [29,30]. Ultimately, a derivation was carried out using the BBGKY hierarchy in the density operator formalism [31]. This required a modification of the typical weak-correlation assumption in derivations of the Boltzmann equation. Instead of neglecting three-body correlations entirely, Boercker and Dufty included the quantum correlations of two scattering particles with a third spectator particle to preserve Fermion antisymmetry, without including correlations due to the interaction. By this method they self-consistently derived the BUU equation with the statistical θ_s factors, but came to the conclusion that the degeneracy must be accounted for in calculating the scattering cross section in addition to influencing the statistical availability of scattering states encapsulated in the θ_s terms.

The BUU equation as originally formulated is applicable to moderately dense gases in which degeneracy is present but the amount of correlation is small. In the case of WDM, the equation has several deficiencies. First, the electron number density and therefore the average ionization state of the system must be provided as an input. Second, in a plasma it is well known that transport rates predicted by Eq. (4) diverge if the cross section is computed using the Coulomb potential because the Coulomb force is of an infinite range. This is typically resolved in an ad hoc manner by enforcing a large distance limit on the impact parameter. Third, the derivation of the BUU equation, while including correlations due to Fermi statistics, does not allow for correlations due to the interaction and thus applies only in the limit of weak coupling. The remainder of this section describes how all three deficiencies can be addressed in a consistent fashion in the WDM regime.

For a tenuous and hot (read classical and weakly coupled) plasma the equilibrium ionization state is determined by the Saha equation [32]]. The divergence in the Coulomb logarithm is related to the neglect of correlation: in plasmas the collective affect of the surrounding plasma introduces Debye screening that limits the range of the interaction. A recent approach called "mean force kinetic theory" has provided a self-consist derivation for plasmas through a new expansion parameter of the BBGKY hierarchy [8]. In standard derivations of the Boltzmann equation, the BBGKY hierarchy is truncated via neglecting correlations involving three or more particles and making certain assumptions about two-particle correlations. In mean-force kinetic theory the BBGKY hierarchy is re-arranged in terms of an expansion parameter that is the difference between the exact nonequilibrium distribution function and its equilibrium limit. The hierarchy is then truncated by assuming this difference is negligible for reduced distribution functions in three or more particle coordinates; i.e. that the high order correlations take their equilibrium values. The result is a collision integral identical in form to that of the Boltzmann equation, but in which the scattering particles interact through the PMF. In addition, there is a term on the left-hand side of the kinetic equation that enforces the nonideality of the equilibrium limit in the equation of state. The result is capable of describing transport in weak to moderately coupled plasmas ($\Gamma \lesssim 20$) based on the equilibrium structural properties of the plasma.

B. The quantum potential of mean force

Extending mean-force kinetic theory to include quantum effects is complicated by two issues: the exclusion principle complicates the mathematics of the necessary statistical averaging, and more significantly the uncertainty principle muddles the very meaning of a potential of mean force. Classically, the mean force is the force experienced between two particles at rest with a given separation, with a statistical averaging over all of the remaining particles in the plasma at equilibrium. In the quantum case, knowing particles are "at rest with a given separation" is impossible according to the uncertainty principle. Mathematically, this prevents factoring of the kinetic and potential (configuration) terms in the equilibrium density matrix, and ultimately prevents a general derivation of the PMF by extension of known classical means.

Despite this complication, the PMF must have some meaning in at least a semiclassical sense. An electron-ion pair will still induce well-defined correlations in the plasma, and these correlations can in turn influence the force felt by the interacting pair at least over the average of many scattering events at many velocities. This is reflected in the screened potential

$$U_{\rm sc}(r) = \frac{\phi(r)}{k_B T} e^{-r/\lambda_{\rm sc}}, \tag{5}$$

with degeneracy-dependent screening length (as per Ref. [9])

$$\lambda_{\rm sc}^2 = \lambda_{\rm D}^2 \sqrt{\frac{{\rm Li}_{3/2}(-\xi)}{{\rm Li}_{1/2}(-\xi)}}, \tag{6}$$

which can be seen as a weak-correlation limit of the PMF both for classical and quantum plasmas. The essential challenge of applying the mean force concept to WDM is how to encapsulate this effect in a binary potential when the coupling is no longer weak. It has long been known that weak correlations influence the potential in the form of plasma screening in both the classical (Debye-Huckel) and quantum (Thomas-Fermi) limits. One other classical derivation of the PMF is via the Ornstein-Zernike equation, which defines the direct correlation function [33]. Fortunately, a quantum analog of the Ornstein-Zernike equation exists (see [34] for its first appearance in the literature to our knowledge), and this equation has been used successfully to calculate the equilibrium pair correlation function in WDM by Starrett and Saumon [18,26,35]. Furthermore, it has been used to define a quantum PMF for electron-ion interactions, and this potential has been used to predict electrical conductivities in the relaxation time approximation, with good agreement with quantum molecular dynamics simulations [36].

Despite the mathematical difficulty in obtaining an expression for the quantum PMF from the quantum BBGKY hierarchy, we postulate that a such a potential must arise naturally from the procedure of rearranging the BBGKY hierarchy as in Ref. [8], and that this potential is that which is derived from the quantum Ornstein-Zernike equation. We turn to such a potential obtained with the quantum hypernetted-chain-approximation, coupled with an average-atom model that accounts for the structure and ionization state of the ions [18,26,35,36] (subsequently referred to as the AA-TCP model for "average-atom two-component plasma." This potential can

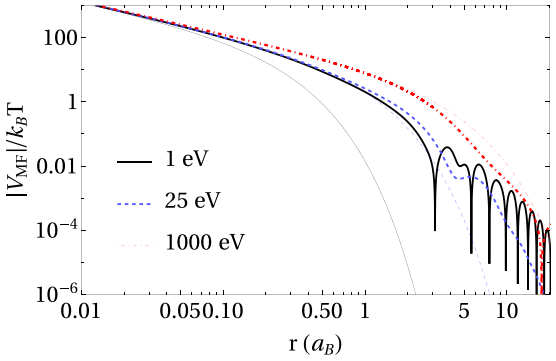

FIG. 2. Electron-ion potential of mean force as obtained via the model described in Ref. [36] for solid-density ($2.7\,\mathrm{g\,cm^{-3}}$) warm dense aluminum at 1, 25, and 500 eV (thick curves). In the high-temperature limit the potential approaches the screened Coulomb potential of a classical plasma (thin curves); as the temperature decreases it is altered by both degeneracy and correlations leading to different scale lengths of the potential in addition to the nonmonotonic behavior.

be expressed as

$$V^{\mathrm{MF}}(r) = -\frac{Z_{\mathrm{nuc}}}{r} + \int d^3r' \frac{n_e^{\mathrm{ion}}(r')}{|\boldsymbol{r}-\boldsymbol{r'}|} + V^{\mathrm{xc}}[n_e^{\mathrm{ion}}(r)] + n_i^0 \int d^3r' \frac{C_{ie}(|\boldsymbol{r}-\boldsymbol{r'}|)}{-\beta} h_{ii}(r') + \bar{n}_e^0 \int d^3r' \frac{C_{ee}(|\boldsymbol{r}-\boldsymbol{r'}|)}{-\beta} h_{ie}(r'), \tag{7}$$

where C_{ie} and C_{ee} are the electron-ion and electron-electron direct correlation functions, respectively, h_{ie} and h_{ii} are the electron-ion and ion-ion pair correlation functions, respectively, $n_e^{\mathrm{ion}}(r)$ is the density of bound electrons, $\beta = k_BT$, and V^{xc} is the exchange correlation functional. V^{xc} may be chosen in accordance with the requirements of the plasma conditions and computational resources available (in the present case, as described in Ref. [26], the zero-temperature Dirac exchange functional [37] is used). In Eq. (7) the first three terms represent the potential for individual ions interacting with free electrons while the last two terms come from the Ornstein-Zernike equation for the electron-ion system. Calculation of the potential requires closure, which in this case is provided by the quantum hypernetted-chain-approximation for the ion-ion correlations and through coupling to an Average-Atom model for the electron-ion correlations. Such methods can be substantially faster than full dynamical calculations such as molecular dynamics, wherein lies the primary benefit of the theory proposed in this work. In Fig. 2 we show example electron-ion scattering potentials from the AA-TCP model for warm dense aluminum at conditions that span the weakly coupled classical to moderately coupled degenerate regimes; see regions (1) and (4) of Fig. 1. The figure demonstrates the convergence of the PMF with a screened Coulomb potential in the weakly coupled limit, and the importance of correlations in the calculation of the potential in the region of moderate coupling.

III. TRANSPORT RATES

Comprehensive methods to derive hydrodynamic equations, such as that of Chapman and Enskog have been developed for the Boltzmann equation [38], but their extension to the BUU equation faces considerable mathematical challenges and has not been accomplished to our knowledge. To demonstrate predictions for macroscopic transport rates, we focus on electron-ion relaxation in which the respective electron and ion distribution functions are known but the species are not in equilibrium with each other. We consider both temperature relaxation and momentum relaxation, which is related to the electrical conductivity. A restriction imposed by considering only electron-ion relaxation is that it provides only one contribution to processes such as electrical conductivity that are also influenced by electron-electron interactions. Although models such as the quantum Landau-Fokker-Planck equation have been solved using a Chapman-Enskog technique to address both contributions in a comprehensive hydrodynamic theory [15], they do not address strong coupling. A recent modification has been proposed to incorporate strong coupling via a modified Coulomb logarithm computed using the PMF and finds that in the strongly degenerate regime and for high-Z systems the electron-ion collisions are dominant [39]. However, the Fokker-Planck form of the collision operator itself is only expected to apply when momentum transfer during collisions is small (i.e., weak coupling). For instance, it can be derived from a small momentum transfer expansion of the BUU equation. Here, we focus on the electron-ion relaxation using the full BUU equation to isolate the influence of large momentum transfer in the collision operator.

Concentrating on the electron-ion contribution also allows for a commensurable comparison with quantum MD simulations of electrical conductivity [28]. Since electrons are often treated using the Born-Oppenheimer approximation in these simulations, they are also limited to treat only the electron-ion contribution to transport processes. Although electron-electron interactions are expected to contribute to the total conductivity, it is only recently becoming possible to go beyond Born-Oppenheimer and simulate dynamic electrons in WDM following advancements in wave-packet MD [40], mixed quantum-classical MD [41,42], Bohmian quantum methods [43], Kohn-Sham DFT MD [44], time-dependent DFT [45] and quantum Monte Carlo [46]. Addressing contributions from both electron and ion dynamics will be the next step in both the theory and simulation development.

A. General formalism

A binary mixture of two species s and s' out of equilibrium will relax towards equilibrium through $s-s$, $s-s'$ and $s'-s'$ collisions, which are modeled by moments of the collision operator Eq. (4),

$$\langle \chi \rangle^{s-s'} = \int d\boldsymbol{v}\, \chi(\boldsymbol{v}) C_{qB}^{s-s'}, \tag{8}$$

where $\chi(\boldsymbol{v})$ is some polynomial function of the velocity. To simplify, we utilize the following properties: $d\Omega \frac{d\sigma}{d\Omega}$ is invariant under reversal of the collision, i.e., $(\boldsymbol{v}, \boldsymbol{v}') \leftrightarrow (\hat{\boldsymbol{v}}, \hat{\boldsymbol{v}}')$ where $\boldsymbol{v}$ and $\boldsymbol{v}'$ are the precollision velocities of particles one

and two, respectively, the "hat" ˆ indicates a post-collision quantity, and the phase-space volume element is invariant, i.e., $\int d\boldsymbol{v}d\boldsymbol{v}' = \int d\hat{\boldsymbol{v}}d\hat{\boldsymbol{v}}'$. We thus obtain

$$\langle\chi\rangle^{s-s'} = \int d\boldsymbol{v}\int d\Omega\frac{d\sigma}{d\Omega}u\int d\boldsymbol{v}'[\chi(\hat{\boldsymbol{v}})-\chi(\boldsymbol{v})] \times f_s f_{s'}\big(1+\theta_s\hat{f}_s\big)\big(1+\theta_s\hat{f}_{s'}\big). \tag{9}$$

Relevant $\chi(v)$ include

$$\chi(\boldsymbol{v}) = \begin{cases} 1 \to [\chi(\hat{\boldsymbol{v}})-\chi(\boldsymbol{v})] = 0, \\ m_s\boldsymbol{v} \to [\chi(\hat{\boldsymbol{v}})-\chi(\boldsymbol{v})] = m_s\boldsymbol{\Delta}v, \\ m_s v^2 \to [\chi(\hat{\boldsymbol{v}})-\chi(\boldsymbol{v})] = m_s\Delta v^2, \end{cases} \tag{10}$$

where $\Delta\boldsymbol{v} = \hat{\boldsymbol{v}}-\boldsymbol{v}$. Substituting variables $\boldsymbol{v} = \boldsymbol{v}'+\boldsymbol{u}$, defining $m_{ss'} = m_s m_{s'}/(m_s+m_{s'})$, and utilizing the following relations obtained from the collision kinematics: $m_s\Delta\boldsymbol{v} = m_{ss'}\Delta\boldsymbol{u}$, $\Delta\boldsymbol{u}\cdot\Delta\boldsymbol{u} = -2\boldsymbol{u}\cdot\Delta\boldsymbol{u}$ and $(2\boldsymbol{v}\cdot\Delta\boldsymbol{v}+\Delta\boldsymbol{v}^2) = (m_{ss'}/m_s)\Delta\boldsymbol{u}\cdot[\boldsymbol{v}'+(m_{ss'}/m_s)\boldsymbol{u}]$, shows that (see Ref. [47]),

$$\chi(\boldsymbol{u}) = \begin{cases} 1 \to [\chi(\hat{\boldsymbol{v}})-\chi(\boldsymbol{v})] = 0, \\ m_s\boldsymbol{v} \to [\chi(\hat{\boldsymbol{v}})-\chi(\boldsymbol{v})] = m_{ss'}\Delta\boldsymbol{u}, \\ m_s v^2 \to [\chi(\hat{\boldsymbol{v}})-\chi(\boldsymbol{v})] = m_{ss'}\big(\boldsymbol{v}'-\boldsymbol{V}_s+\frac{m_{ss'}}{m_{s'}}\boldsymbol{u}\big)\cdot\Delta\boldsymbol{u}, \end{cases} \tag{11}$$

where

$$\Delta\boldsymbol{u} = u\bigg(\sin\theta\cos\phi\hat{\boldsymbol{x}}+\sin\theta\sin\phi\hat{\boldsymbol{y}}-2\sin^2\frac{\theta}{2}\hat{\boldsymbol{u}}\bigg). \tag{12}$$

With this expression it is easy to verify the useful identity

$$(\boldsymbol{u}+\boldsymbol{\Delta u})^2 = u^2. \tag{13}$$

The preceding discussion and the collision operator Eq. (4) are in principle applicable to transport in any semiclassical system. As it pertains to WDM, ion-ion scattering is contained within this formalism as ion dynamics are classical and electron degeneracy effects enter only via the PMF. Application of the theory to ion-ion scattering was validated in Ref. [14]. The case of the electron-electron terms requires further work due to the subtleties associated with defining the PMF that are discussed in section II and will be investigated in another work. However, the model at the level to which we have developed it has immediate applicability to the case of electron-ion scattering.

B. The relaxation problem

We restrict our analysis to the class of problems in which electrons and ions in the plasma are in respective equilibrium with themselves with different fluid quantities T_e, T_i, $\boldsymbol{V}_e$, and $\boldsymbol{V}_i$, respectively. In such a system, the electron and ion fluid variables will equilibrate on a timescale long compared to the respective electron-electron and ion-ion collision times. The ions have a classical Maxwellian velocity distribution,

$$f_i(\boldsymbol{v}') = \frac{n_i}{v_{Ti}^3}\frac{e^{-(\boldsymbol{v}'-\boldsymbol{V}_i)^2/v_{Ti}^2}}{\pi^{3/2}}, \tag{14}$$

and the electrons have a Fermi-Dirac velocity distribution

$$f_e(\boldsymbol{v}) = n_e\bigg[v_{Te}^3\big(-\pi^{3/2}\mathrm{Li}_{\frac{3}{2}}(-\xi)\big)\bigg(1+\frac{e^{(\boldsymbol{v}-\boldsymbol{V}_e)^2/v_{Te}^2}}{\xi}\bigg)\bigg]^{-1}, \tag{15}$$

where $v_{Ts} = \sqrt{2k_BT_s/m_s}$ and $\xi = \exp(\mu/k_BT)$, the ion velocity is $\boldsymbol{v}'$ and electron velocity is $\boldsymbol{v}$. We can write

$$\begin{aligned} &f_e f_i(1+\theta_e\hat{f}_e) \\ &= \frac{n_i}{v_{Ti}^3}\frac{e^{-(\boldsymbol{v}'-\boldsymbol{V}_i)^2/v_{Ti}^2}}{\pi^{3/2}}n_e \\ &\quad\times\bigg[v_{Te}^3\big(-\pi^{3/2}\mathrm{Li}_{\frac{3}{2}}(-\xi)\big)\bigg(1+\frac{e^{(\boldsymbol{v}'+\boldsymbol{u}-\boldsymbol{V}_e)^2/v_{Te}^2}}{\xi}\bigg)\bigg]^{-1} \\ &\quad\times\bigg[1-\bigg(1+\frac{e^{(\boldsymbol{v}'+\boldsymbol{u}+(m_{ei}/m_e)\Delta\boldsymbol{u}-\boldsymbol{V}_e)^2/v_{Te}^2}}{\xi}\bigg)^{-1}\bigg], \end{aligned} \tag{16}$$

from which the relation of the factor $(1+\theta_e\hat{f}_e)$ to Pauli blocking can be seen in terms of the Fermi-Dirac occupation number: the contribution to the collision integral from collisions to or from occupied states is zero. This simplification occurs from the combination of $\theta_e = (-1/2)(h/m_s)^3$ with the prefactor $n_e v_{Te}^3/\mathrm{Li}_{\frac{3}{2}}(-\xi)$ in the Fermi Dirac distribution through the relation Eq. (3).

Electron-ion temperature and momentum relaxation rates depend on the energy exchange density $Q^{s-s'}$ and friction force density $\boldsymbol{R}^{s-s'}$, respectively. These can in turn be written in terms of the moments Eq. (9), assuming a uniform plasma, as

$$Q^{ei} = \big\langle\tfrac{1}{2}m_e(\boldsymbol{v}-\boldsymbol{V}_e)^2\big\rangle^{e-i} \tag{17}$$

and

$$\boldsymbol{R}^{ei} = \langle m_e\boldsymbol{v}\rangle^{e-i}, \tag{18}$$

which, in the respective limits of $\Delta T = T_e - T_i \ll T$ and $\Delta V = V_e - V_i \ll V$, yield simple relaxation rates $dT_e/dt = \nu_{ei}^{(\epsilon)}\Delta T$ and $d\boldsymbol{V}_e/dt = \nu_{ei}^{(p)}\Delta\boldsymbol{V}$.

The integration over the ion velocity can be simplified significantly in the limit that the ion velocities are much smaller than the electron velocities: $m_eT_i \ll m_iT_e$, which (due to the small electron-to-ion mass ratio) is true when temperature differences are not extreme, coinciding with our expansion about the equilibrium state. Note that we also make the simplifying replacement $m_{ei} \approx m_e$. By expanding Eq. (16) in the limit that the electron distribution is approximately constant over the range of accessible ion velocities, the integral over the ion velocities can be carried out analytically. The evaluation of this integral differs for the calculation of Q^{ei} versus $\boldsymbol{R}^{ei}$. Therefore we examine each case separately.

1. Temperature relaxation

The energy-exchange density Eq. (17) in this case becomes

$$Q^{ei} = m_{ei}\int d\boldsymbol{u}\int d\Omega\frac{d\sigma}{d\Omega}u\boldsymbol{\Delta u} \times\int d\boldsymbol{v}'\bigg(\boldsymbol{v}'+\frac{m_{ei}}{m_i}\boldsymbol{u}\bigg)f_i f_e\big(1-|\theta_e|\hat{f}_e\big). \tag{19}$$

Inserting Eq. (16), applying the expansion $|\boldsymbol{v}'| \ll |\boldsymbol{u}|$, assuming zero drift velocities and $|T_e - T_i| \ll T_e, T_i$ and using Eq. (13) we perform the integral over $\boldsymbol{v}'$ and write

$$\int d\boldsymbol{v}'\left(\boldsymbol{v}' + \frac{m_{ei}}{m_i}\boldsymbol{u}\right) f_i f_e (1 - |\theta_e|\hat{f}_e) \approx \frac{m_e}{m_i}\frac{n_e n_i e^{-u^2/v_{Te}^2}\xi \boldsymbol{u}}{\pi^{3/2} v_{Te}^3 (1 + \xi e^{-u^2/v_{Te}^2})^2 \mathrm{Li}_{\frac{3}{2}}(-\xi)}. \quad (20)$$

The result is written to facilitate comparison with the classical limit,

$$Q^{ei} = -3\frac{m_e}{m_i} n_e \nu_{ei}(T_e - T_i), \quad (21)$$

in terms of a collision frequency

$$\nu_{ei} = \nu_0 \Xi_{ei}, \quad (22)$$

where

$$\nu_0 \equiv \frac{4\sqrt{2\pi} n_i Z^2 e^4}{3\sqrt{m_e}(k_B T_e)^{3/2}} = 2.906 \times 10^{-12} \frac{Z n_i [\mathrm{m}^{-3}]}{(T_e[\mathrm{eV}])^{3/2}} \quad (23)$$

and a generalized Coulomb integral Ξ_{ei}. Effects of degeneracy and strong coupling are contained in the Coulomb integral,

$$\Xi_{ei} = \frac{1}{2}\int_0^\infty d\eta I(\eta) \quad (24)$$

$$I(\eta) \equiv G(\eta)\frac{\sigma^{(1)}(\eta, \Gamma)}{\sigma_0}, \quad (25)$$

where $\eta \equiv u/v_{Te}$ and

$$\sigma^{(1)}(\eta, \Gamma) = 4\pi \int_0^\pi d\theta \sin^2\frac{\theta}{2} \sin\theta \frac{d\sigma}{d\Omega} \quad (26)$$

is the momentum transfer cross section, which can be written in terms of the phase shifts δ_l as

$$\frac{\sigma^{(1)}}{\sigma_0} = \frac{4\pi}{\eta^2}\sum_{l=0}^\infty (l+1)\sin^2(\delta_{l+1} - \delta_l), \quad (27)$$

with a convenient reference cross section being the squared thermal de Broglie wavelength $\sigma_0 = \hbar^2/(m_e v_{Te})^2$. The function

$$G(\eta) \equiv \frac{\xi e^{-\eta^2}\eta^5}{[-\mathrm{Li}_{\frac{3}{2}}(-\xi)](\xi e^{-\eta^2} + 1)^2} \quad (28)$$

determines the relative availability of states that contribute to the scattering. This is plotted in Fig. 3 for several values of the degeneracy parameter Θ, where it is shown that in the classical limit scattering is dominated by energy transfers around the thermal energy, and as degeneracy increases the envelope of relevant energy-transfers narrows about the Fermi energy. It should be noted that the relaxation rate obtained in Eq. (22) is identical to that obtained in Eq. (71) of Ref. [27] by very different means.

2. Momentum relaxation

Momentum relaxation occurs through collisions between electron and ion populations with different average velocities.

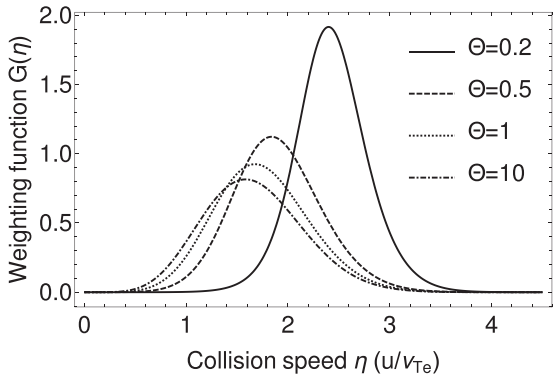

FIG. 3. Statistical weighting function G from the integrand for temperature and momentum relaxation, spanning the transition from classical to degenerate conditions. The relevant collision velocities become narrowly centered around the Fermi velocity at strong degeneracy. This represents the availability of regions of phase space for scattering particles to leave/enter, with the Pauli principle greatly restricting the available states at collision energies below the Fermi energy when the plasma is degenerate.

The force density Eq. (18) associated with these collisions is

$$\boldsymbol{R}^{ei} = \int d\boldsymbol{u}\int d\Omega \frac{d\sigma}{d\Omega} u \int d\boldsymbol{v}' m_{ei}\Delta\boldsymbol{u} f_e f_i (1 + \theta_e \hat{f}_e). \quad (29)$$

Inserting Eq. (16), again applying the expansion $|\boldsymbol{v}'| \ll |\boldsymbol{u}|$, identity 13, and assuming $|T_e - T_i| \ll T_e, T_i$, $V_i \ll v_{Ti}$ and $V_e \ll v_{Te}$, the integral over $\boldsymbol{v}'$ can be performed analytically,

$$\int d\boldsymbol{v}' m_{ei} f_e f_i (1 + \theta_e \hat{f}_e) \approx \frac{2 m_e n_e n_i \xi e^{-\eta^2}[\boldsymbol{u}\cdot\Delta\boldsymbol{V}(1 - \xi e^{-\eta^2}) - \xi e^{-\eta^2}\Delta\boldsymbol{u}\cdot\Delta\boldsymbol{V}]}{\pi^{3/2} v_{Te}^5 [-\mathrm{Li}_{\frac{3}{2}}(-\xi)](\xi e^{-\eta^2} + 1)^3}. \quad (30)$$

The remaining integrals are simplified by choosing a coordinate system aligned with $\Delta\boldsymbol{V}$ in which $\hat{\boldsymbol{u}} = \sin\theta'\cos\phi'\hat{\boldsymbol{x}} + \sin\theta'\sin\phi'\hat{\boldsymbol{y}} + \cos\theta'\Delta\hat{\boldsymbol{V}}$ and additionally rotating $\Delta\boldsymbol{u}$ into this coordinate system. We follow the classical example and write the resulting expression in the form

$$\boldsymbol{R}^{ei} = -n_e m_e \nu_{ei}(\boldsymbol{V}_e - \boldsymbol{V}_i), \quad (31)$$

where the frequency ν_{ei} is the same that appears in the case of temperature relaxation in Eq. (22). It is interesting to note that Eq. (30) contains a term that is nonlinear in the momentum exchange $m_e\Delta\boldsymbol{u}$ and thus contains effects due to large angle collisions. The quantum Landau-Fokker-Planck equation results from the small collision angle limit of the BUU equation and thus neglects this term, leading to a different expression. Since this term vanishes when $\xi \to 0$, in the classical limit the Boltzmann and Landau-Fokker-Planck equations have the same momentum moment [48].

3. Electrical conductivity

The electrical conductivity is an important transport coefficient that depends largely on the electron-ion collisional momentum relaxation rate. Considering a Fermi-Dirac electron population flowing through a stationary Maxwellian ion

population due to an applied electric field, the frictional force balances the electric force

$$\boldsymbol{R}_{ei} = -en_e\boldsymbol{E}, \tag{32}$$

which in the form of Eq. (31) is connected to the current through Ohm's law,

$$\boldsymbol{J} = \sigma\boldsymbol{E}, \tag{33}$$

where $\boldsymbol{J} = -en_e\boldsymbol{V}_e$. Using the electron-ion collisional friction [Eq. (31)], the resulting electrical conductivity is

$$\sigma = \frac{e^2 n_e}{m_e \nu_{ei}}, \tag{34}$$

where ν_{ei} is defined in Eq. (22). The assumption of a Fermi-Dirac electron distribution means that electron-electron (e-e) collisions do not contribute to the relaxation; distortions in the electron distribution away from equilibrium amount to a higher-order approximation that could be explored, e.g., through the Chapman-Enskog expansion. The e-e collisions do not contribute substantially in the degenerate regimes due to Pauli blocking, and at high temperatures the e-e contribution is well understood via the Landau-Spitzer theory. The intermediate regime where both degeneracy and e-e collisions are important is discussed by Shaffer and Starrett [39] in the context of the quantum Fokker-Planck equation. The application of the BUU equation to this regime to relax the assumption of small-momentum-transfer collisions will require a Chapman-Enskog expansion of the BUU equation and will be addressed in further studies.

IV. RESULTS AND DISCUSSION

To illustrate the application of the model, we now turn to evaluating it, with input potentials provided by the AA-TCP model [26,35] for aluminum at a density of 2.7 g cm^{-3}, over a range of temperatures spanning from the degenerate moderately coupled to classical weakly coupled regimes. The phase shifts are obtained as described in the Appendix, and the numerical integration limits over the relative velocity η are determined by considering the range over which the weighting function Eq. (28) is larger than 10^{-6}.

A. Relaxation rates in solid density aluminum plasma

Figure 4 shows a comparison of the reference electron-ion relaxation rate computed from different models. Standard models include the well-established Landau-Spitzer result [10], which in the limit $m_e T_i \ll m_i T_e$ reduces to

$$\nu_{ei}^{\mathrm{LS}} \approx \nu_0 \ln\Lambda_{\mathrm{LS}}, \tag{35}$$

which has been verified in the classical limit given sufficiently weak coupling [49,50]. The relaxation rate predicted by the LFP model is (see Eqs. (14)– (17) of Ref. [11]),

$$\nu_{ei}^{\mathrm{LFP}} = \nu_0\left(\ln\Lambda_{\mathrm{LFP}}\frac{\xi}{1+\xi}\frac{3\sqrt{\pi}\Theta^{3/2}}{4}\right). \tag{36}$$

We further note that our expression for the temperature relaxation rate [given by Eqs. (21)–(27)] is the same as that recently obtained by a substantially different approach by Daligault and Simoni (see Eqs. (71)–(75) of Ref. [27]) if the PMF is used for calculating the transport cross section there. This equivalency can be seen through use of the relation $n_e(h/\sqrt{\pi}m_e v_{Te})^3 = -2\mathrm{Li}_{3/2}(-\xi)$ from the normalization of the Fermi-Dirac distribution.

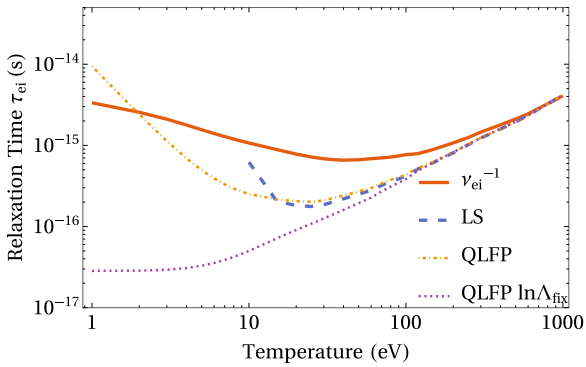

FIG. 4. Electron-ion collisional relaxation times ($\tau = \nu_{ei,}^{-1}$) as a function of temperature in solid density (2.7 g cm^{-3}) aluminum. This demonstrates the influence of different physical effects, as the LFP equation does not contain effects due to strong coupling or strong scattering, and the Landau-Spitzer theory additionally does not account for electron degeneracy in the scattering physics.

At a given density, as temperature decreases the Coulomb logarithm will eventually reach zero due to neglect of strong coupling physics. The resulting divergence of the Landau-Spitzer result is due to the presence of the (inverse) Coulomb logarithm

$$\ln\Lambda_{\mathrm{LS}} = \ln\frac{b_{\max}}{b_{\min}}. \tag{37}$$

The maximum impact parameter is modeled as the larger of the screening length λ_{sc} [Eq. (6)] or the Wigner-Seitz radius $a = (3/4\pi n_i)^{1/3}$, and the minimum is the larger of the classical distance of closest approach $r_L = e^2/k_B T$ or the thermal de Broglie wavelength $\lambda_{\mathrm{dB}} = \hbar/(m_e k_{\mathrm{B}} T_e)^{1/2}$ [17]. In WDM, the vanishing Coulomb logarithm is often resolved through the modification (see, e.g., Ref. [17])

$$\ln\Lambda_{\mathrm{LFP}} = \frac{1}{2}\ln\left(1+\frac{b_{\max}^2}{b_{\min}^2}\right), \tag{38}$$

which we apply in our evaluation of the LFP model. This is often further altered, as is done in the Lee-More conductivity model [17], by enforcing that the minimum value of the Coulomb logarithm be 2:

$$\ln\Lambda_{\mathrm{fix}} = \max\left[2, \frac{1}{2}\ln\left(1+\frac{b_{\max}^2}{b_{\min}^2}\right)\right]. \tag{39}$$

The approximations inherent in this approach are two-fold: small-angle collisions must be assumed to obtain the LFP equation, and the choice of maximum and minimum impact parameters represents an uncontrolled expansion in the strongly coupled regime. The convergent kinetic equation in our approach avoids these limitations.

Figure 4 confirms the expectation that all expressions agree at high temperatures associated with the weakly coupled classical regime, while at low temperature the models differ as a result of the different levels of inclusion of the physics

of strong coupling and degeneracy. In each case there is a minimum in the relaxation time. In all cases except the Landau-Spitzer result, this minimum can be attributed to a combination of both degeneracy and strong coupling: strong coupling increases the collisionality of the system while the onset of degeneracy reduces the collisionality through Pauli blocking. The decreased level of ionization at lower temperatures also reduces the collisionality. If the density is less than $10^{23}\,\mathrm{cm}^{-3}$ as temperature is reduced the plasma will first become strongly coupled and then degenerate, and if the density is greater than $10^{23}\,\mathrm{cm}^{-3}$ the electrons will be degenerate when the transition to strong coupling occurs.

The term proportional to $(\Delta u)^2$ in Eq. (29) is a result of large-angle collisions, and is thus not present in the LS or QLFP theories. The LS and QLFP theories also do not account for correlations in the plasma beyond the assumed presence of a screening length. The LS theory ignores both degeneracy and large-angle scattering. The QLFP theory extends further into the degenerate regime and has fixed the vanishing Coulomb log, but does not account for either correlations or large-angle scattering when there is strong Coulomb coupling. The divergence between the QLFP results using the two different prescriptions for the Coulomb log illustrates the lack of strong-coupling physics in the method.

B. Electrical conductivity of solid-density aluminum plasma

We proceed to evaluate the electrical conductivity according to Eq. (34) for aluminum at $2.7\,\mathrm{g\,cm}^{-3}$, as a demonstration of the model in a regime marked by partial ionization and a simultaneous transition from weak to strong coupling and classical to degenerate statistics. For comparison we select the Lee-More model, the model of Shaffer and Starrett [39] and the QMD simulations of Witte *et al.* [28]. The electrical conductivity coefficient predicted by the LM model [17] is

$$\sigma_e = \frac{ne^2}{m}\left\{\frac{3\sqrt{m}(kT)^{3/2}}{2\sqrt{2}\pi Z^2 n_i e^4 \ln\Lambda_{\mathrm{fix}}}\right\}\frac{4}{3}\frac{\int_0^\infty \frac{t^2 dt}{1+\exp(t-\mu/kT)}}{\int_0^\infty \frac{t^{1/2} dt}{1+\exp(t-\mu/kT)}}, \quad (40)$$

which we relate to the friction force density $\boldsymbol{R}$ and thus the scattering rate, $\nu_{ei} = e^2 n_e/\sigma m_e$, giving

$$\nu_{ei}^{\mathrm{LM}} = \nu_0\left[\ln\Lambda_{\mathrm{fix}}\frac{\mathrm{Li}_{3/2}(-\xi)}{\mathrm{Li}_3(-\xi)}\right]. \quad (41)$$

The Starrett and Shaffer model similarly uses the quantum PMF to mediate scattering, but in the context of the QLFP equation. To introduce the effect of large-angle collisions into the model they introduce a Coulomb logarithm defined via the relaxation-time approximation (RTA) which we will refer to as $\ln\Lambda_{\mathrm{SS}}$. For a commensurate comparison with our method (where we assume a Fermi distribution for the electrons) and the QMD simulations, we neglect the higher-order Chapman-Enskog corrections associated with electron-electron interactions that can be obtained in the SS model. The electron-ion contribution corresponds with the first order of the Chapman-Enskog expansion,

$$\sigma_{1,\mathrm{qLFP}} = \frac{3(4\pi\epsilon_0)^2(k_B T)^{3/2}}{4\sqrt{2\pi m_e}Ze^2\ln\Lambda_{\mathrm{ss}}}\frac{\mathrm{Li}_{3/2}(-\xi)}{\mathrm{Li}_0(-\xi)}. \quad (42)$$

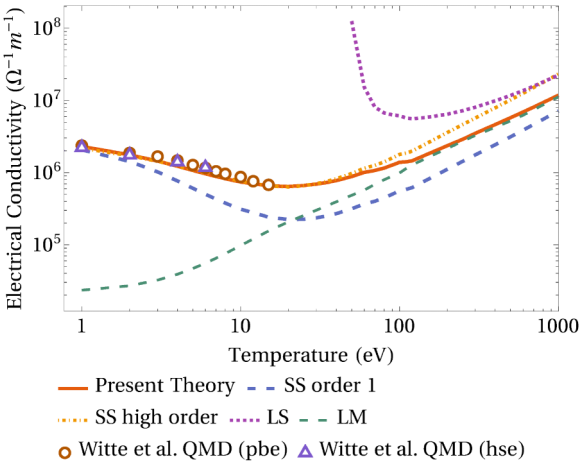

FIG. 5. Electron-ion contribution to the electrical conductivity of solid density aluminum ($2.7\,\mathrm{g\,cm}^{-3}$) as derived through the current work (solid line) the Starrett and Shaffer model evaluated at first order (dashed line) and at high order (dot-dashed line) in the Chapman-Enskog expansion, the Lee-More model (thin dashes), the LS conductivity (dotted line), along with QMD results of Witte *et al.* [28] using the Perdew–Burke-Ernzerhof and Heyd–Scuseria–Ernzerhof exchange-correlation functionals.

With the identification of

$$\mathrm{Li}_0(-\xi) = \frac{-\xi}{1+\xi} \quad (43)$$

and [from Eq. (36)]

$$\ln\Lambda\frac{\xi}{1+\xi}\frac{3\sqrt{\pi}\Theta^{3/2}}{4} \to \ln\Lambda, \quad (44)$$

and Eq. (3) it can be seen that this is equivalent in form to Eq. (34) with the difference being the Coulomb logarithm.

The resulting predictions for the conductivity are shown in Fig. 5. Similarly to the relaxation times, there is a minimum in the conductivity near the Fermi temperature. This again can be attributed to both correlations and Pauli blocking [39]. Also as in the case of the relaxation times, the LS theory fails to accurately predict the conductivity when degeneracy and correlations are important, as expected. Furthermore, the commonly used Lee-More theory performs poorly as a result of the correlations. Interestingly, the Lee-More theory can be reproduced by replacing the Coulomb logarithm in the standard QLFP formulation with the fixed version prescribed in the Lee-More theory. Although we focus on the electron-ion contribution, it is known that electron-electron interactions cause a contribution of comparable magnitude in the classical weakly coupled limit (the Spitzer correction) [10]. However, it can be expected that e-e collisions will be greatly suppressed below the Fermi temperature due to Pauli blocking and therefore the corrections due to a higher-order Chapman Enskog expansion will be diminished at lower temperatures. Indeed, this is seen for the QLFP equation [15].

More interesting are the comparisons of the present theory with the Shaffer-Starrett formulation of the QLFP theory [39] and with the QMD simulations of Witte *et al.* [28]. The QLFP equation corresponds to the limit of the BUU equation in which the distribution functions are expanded in the limit of

small momentum transfer in a collision, and the scattering cross section is evaluated in the limit of weak coupling. As such, it may expected that these formulations should agree in the limit of weak coupling. However, the present theory and the SS theory differ in their incorporation of the potential of mean force, and the curves appear to not yet have reached this limiting behavior at 1000 eV. The QMD simulations also make an interesting direct comparison. QMD simulations do not directly include e-e collisions but account for some level of the electronic interactions through the mean field [51]. Thus, it seems most appropriate to compare the QMD simulations with theories evaluated to treat only the electron-ion interactions, as is done in Fig. 5. Indeed, the agreement with these simulations is remarkable for most of the range of available data, even down to 1 eV where it is unclear whether the BUU equation can be expected to be valid as higher-order quantum correlations come into play.

The good agreement between QMD and the BUU predictions provides evidence that large momentum transfer collisions and their associated contribution to the momentum scattering rate are real and significant effects influencing the electrical conductivity. This points to important physics beyond what is captured by the QLFP theory, or its modifications, as is shown by comparing with the first-order Chapman-Enskog solution of the Shaffer-Starrett model from [39] (the first order of this method is equivalent to the electron-ion relaxation model described in the previous section and therefore provides a commensurate comparison). At the same time, it is also important to note deviations of the distribution functions away from their equilibrium profiles are possible and lead to contributions from electron-electron collisions that influence the total conductivity at these conditions. Shaffer and Starrett predict these to make order-unity contributions over most of the range of conditions plotted in Fig. 5 [39], while this contribution is diminished in the degenerate limit as the exclusion principle restricts electron-electron scattering as well as deviations away from the Fermi-Dirac function. This can be seen in the comparison of first order and high order Chapman-Enskog curves of SS. Interestingly, there is strong agreement between the high order SS curve and the BUU curve obtained by our method. This can be attributed in part to the definition of the SS Coulomb log which is obtained in the relaxation time approximation of the BUU equation. However, the SS method still differs in the physics involved: (1) it does not contain the effect of large-angle collisions in the distribution functions which are retained in the BUU equation, but (2) it carries more accurate information about the distribution functions due to Chapman-Enskog. The good agreement between the two methods at low temperatures is thus likely a coincidence arising from the competition of these two effects. Further development will be required to evaluate this effect (for instance a full Chapman-Enskog solution of the BUU equation), as well as to provide a conclusive test using QMD.

V. CONCLUSIONS

We have presented a model for transport in plasmas with weak to moderate Coulomb coupling and weak to moderate electron degeneracy. The model is based on the quantum Boltzmann equation of Uehling and Uhlenbeck, in which the two-body scattering is mediated by the equilibrium potential of mean force. This incorporates correlations in the equilibrium limit while maintaining the simplicity of binary collisions in the dynamical equation. This is relevant to electron-ion collisions in WDM. As input into the model, we utilized an existing model for the potential of mean force derived from the quantum Ornstein-Zernike equations and an average-atom quantum hypernetted-chain-approximation model [18,26,35].

The model was used to compute momentum and energy relaxation rates. The transport coefficients were written analogously to the classical Landau-Spitzer (LS) result in terms of a "Coulomb integral" that takes the place of the traditional Coulomb logarithm. The Coulomb integral depends on the level of degeneracy, and Coulomb coupling enters through the calculation of the momentum-transfer cross section solving the Schrödinger equation with the PMF as the scattering potential. The momentum relaxation rate was found to contain a term with nonlinear dependence on the momentum exchange. In the classical limit this term vanishes and large angle collisions only influence the relaxation rate through their presence in the transport cross section.

We concluded by calculating the temperature and momentum relaxation rates and electrical conductivity in solid density aluminum plasma over a range of temperatures that covered the transitions between weak and moderate coupling and weak and moderate degeneracy. Predictions were compared with other leading models. It was found that all models behave as expected in the classical weak-coupling limit, and diverge widely in the limit of a degenerate moderately coupled plasma. We assessed the relative importance of the different relevant physical processes that complicate the problem as degeneracy and coupling simultaneously increase: diffraction, Pauli blocking, correlations, and large-angle scattering.

This work can be improved through inclusion of electron-electron collisions and higher-order terms of a Chapman-Enskog expansion. Additionally, further work will be required to obtain a rigorously derived convergent kinetic equation with the appropriate potential of mean force. Ultimately, current and near-future experimental measurements [1,52,53] and *ab initio* simulations [40–46] will be needed for discrimination between the validity of the various models of relaxation in WDM. This will enhance our understanding of the basic physics of WDM, and allow increased fidelity in the rapid calculation of transport coefficients for use in hydrodynamic simulations of naturally and experimentally occurring WDM.

ACKNOWLEDGMENTS

The authors acknowledge Charles Starrett and Nathaniel Shaffer for the provision of input data at equilibrium for the potential of mean force and for their valuable comments on this work. This material is based upon work supported by the U.S. Department of Energy, Office of Science, Office of Fusion Energy Sciences under Award No. DE-SC0016159.

APPENDIX: DETERMINATION OF PHASE SHIFTS

Solution of the scattering problem comes down to solution of the radial Schrödinger equation [54],

$$\frac{d^2u_l}{dr^2} + \left[k^2 - \frac{l(l+1)}{r^2} - \frac{2m_{ei}}{\hbar^2}V(r)\right]u_l = 0,$$

with potential V, wave number k, and angular quantum number l. Cross sections are calculated in the partial wave expansion [55]

$$\frac{d\sigma}{d\Omega} = \left|\frac{1}{2ik}\sum_{l=0}^{\infty}(2l+1)\left(e^{2i\delta_l}-1\right)P_l(\cos\theta)\right|^2, \tag{A1}$$

in terms of the phase shifts δ_l. Using the properties of the Legendre polynomials P_l the transport cross section can be expressed as a sum over phase shifts:

$$\begin{aligned}\frac{\sigma^{(1)}}{\sigma_0} &= 4\pi\int_0^{\pi} d\theta \sin^2\frac{\theta}{2}\sin\theta\frac{d\sigma}{d\Omega}\\ &= \frac{4\pi}{\eta^2}\sum_{l=0}^{\infty}(l+1)\sin^2(\delta_{l+1}-\delta_l).\end{aligned} \tag{A2}$$

The phase shifts can be extracted from the asymptotic behavior of the wave function u_l beyond the range of the potential at point R (defined as a point beyond with the influence of the potential on the wave function is negligible) through the relation:

$$\tan\delta_l = \frac{kRj_l'(kR) - \beta_l j_l(kR)}{kRy_l'(kR) - \beta_l y_l(kR)} \tag{A3}$$

with

$$\beta_l = \frac{1}{u_l/r}\frac{d(u_l/r)}{dr}\bigg|_{r=R}, \tag{A4}$$

where j_l (y_l) are the spherical Bessel (Neumann) functions. For $l > 30$ it is faster and still accurate to use the WKB phase shifts [54]

$$\begin{aligned}\delta_l^{(\mathrm{WKB})} = &-\int_{(l+1/2)/k}^{\infty}\sqrt{k^2 - \frac{(l+1/2)^2}{r^2}}dr\\ &+\int_{r_C}^{\infty}\sqrt{k^2 - \frac{(l+1/2)^2}{r^2} - \frac{2m_e}{\hbar^2}U(r)}dr,\end{aligned} \tag{A5}$$

where r_C the largest root of the function inside the radical in the last term.

[1] S. H. Glenzer, L. B. Fletcher, E. Galtier, B. Nagler, R. Alonso-Mori, B. Barbrel, S. B. Brown, D. A. Chapman, Z. Chen, C. B. Curry, F. Fiuza, E. Gamboa, M. Gauthier, D. O. Gericke, A. Gleason, S. Goede, E. Granados, P. Heimann, J. Kim, D. Kraus *et al.*, J. Phys. B: At. Mol. Opt. Phys. **49**, 092001 (2016).

[2] D. Riley, Plasma Phys. Controlled Fusion **60**, 014033 (2018).

[3] A. Mančić, J. Phys.: Conf. Ser. **257**, 012009 (2010).

[4] R. Redmer, N. Nettelmann, B. Holst, A. Kietzmann, and M. French, Quantum molecular dynamics simulations for warm dense matter and applications in astrophysics, in *Condensed Matter Physics in the Prime of 21st Century: Phenomena, Materials, Ideas, Methods—43rd Karpacz Winter School of Theoretical Physics* (World Scientific, Singapore, 2008), pp. 223–236.

[5] M. Koenig, A. Benuzzi-Mounaix, A. Ravasio, T. Vinci, N. Ozaki, S. Lepape, D. Batani, G. Huser, T. Hall, D. Hicks, A. MacKinnon, P. Patel, H. S. Park, T. Boehly, M. Borghesi, S. Kar, and L. Romagnani, Plasma Phys. Controlled Fusion **47**, B441 (2005).

[6] S. X. Hu, V. N. Goncharov, T. R. Boehly, R. L. McCrory, S. Skupsky, L. A. Collins, J. D. Kress, and B. Militzer, Phys. Plasmas **22**, 056304 (2015).

[7] E. A. Uehling and G. E. Uhlenbeck, Phys. Rev. **43**, 552 (1933).

[8] S. D. Baalrud and J. Daligault, Phys. Plasmas **26**, 082106 (2019).

[9] D. B. Melrose and A. Mushtaq, Phys. Rev. E **82**, 056402 (2010).

[10] L. Spitzer, *Physics of Fully Ionized Gases* (Interscience Publishers, New York, 1956).

[11] J. Daligault, Phys. Plasmas **23**, 032706 (2016).

[12] S. D. Baalrud and J. Daligault, Phys. Rev. Lett. **110**, 235001 (2013).

[13] S. D. Baalrud and J. Daligault, Phys. Plasmas **21**, 055707 (2014).

[14] J. Daligault, S. D. Baalrud, C. E. Starrett, D. Saumon, and T. Sjostrom, Phys. Rev. Lett. **116**, 075002 (2016).

[15] J. Daligault, Phys. Plasmas **25**, 082703 (2018).

[16] D. O. Gericke, M. S. Murillo, and M. Schlanges, Phys. Rev. E **65**, 036418 (2002).

[17] Y. T. Lee and R. M. More, Phys. Fluids **27**, 1273 (1984).

[18] C. E. Starrett, Phys. Plasmas **25**, 092707 (2018).

[19] J. Daligault and G. Dimonte, Phys. Rev. E **79**, 056403 (2009).

[20] M. Lampe, Phys. Rev. **170**, 306 (1968).

[21] C. R. Scullard, S. Serna, L. X. Benedict, C. L. Ellison, and F. R. Graziani, Phys. Rev. E **97**, 013205 (2018).

[22] L. S. Brown, D. L. Preston, and R. L. Singleton, Jr., Phys. Rep. **410**, 237 (2005).

[23] L. S. Brown and R. L. Singleton, Jr., Phys. Rev. E **76**, 066404 (2007).

[24] K. Balzer and M. Bonitz, *Nonequilibrium Green's Functions Approach to Inhomogeneous Systems*, Lecture Notes in Physics, Vol. 867 (Springer, Berlin, 2013).

[25] M. Bonitz, *Quantum Kinetic Theory* (Springer, Cham, Switzerland, 2016).

[26] C. E. Starrett and D. Saumon, Phys. Rev. E **87**, 013104 (2013).

[27] J. Daligault and J. Simoni, Phys. Rev. E **100**, 043201 (2019).

[28] B. B. L. Witte, P. Sperling, M. French, V. Recoules, S. H. Glenzer, and R. Redmer, Phys. Plasmas **25**, 056901 (2018).

[29] D. K. Hoffman, J. J. Mueller, and C. F. Curtiss, J. Chem. Phys. **43**, 2878 (1965).

[30] S. Imam-Rahajoe and C. F. Curtiss, J. Chem. Phys. **47**, 5269 (1967).

[31] D. B. Boercker and J. W. Dufty, Ann. Phys. **119**, 43 (1979).

[32] M. N. Saha, Proc. R. Soc. Lond. A **99**, 135 (1921).

[33] J. Hansen and I. McDonald, *Theory of Simple Liquids*, 3rd ed. (Academic Press, Oxford, 2006).

[34] J. Chihara, J. Phys.: Condens. Matter **3**, 8715 (1991).

[35] C. E. Starrett and D. Saumon, Phys. Rev. E **85**, 026403 (2012).
[36] C. E. Starrett, High Energy Density Phys. **25**, 8 (2017).
[37] P. A. M. Dirac, Proc. Cambridge Philos. Soc. **26**, 376 (1930).
[38] S. Chapman and T. G. Cowling, *The Mathematical Theory of Non-Uniform Gases*, 3rd ed. (Cambridge University Press, Cambridge, UK, 1970).
[39] N. R. Shaffer and C. E. Starrett, Phys. Rev. E **101**, 053204 (2020).
[40] Q. Ma, J. Dai, D. Kang, M. S. Murillo, Y. Hou, Z. Zhao, and J. Yuan, Phys. Rev. Lett. **122**, 015001 (2019).
[41] J. Simoni and J. Daligault, Phys. Rev. Lett. **122**, 205001 (2019).
[42] J. Daligault and D. Mozyrsky, Phys. Rev. B **98**, 205120 (2018).
[43] B. Larder, D. O. Gericke, S. Richardson, P. Mabey, T. G. White, and G. Gregori, Sci. Adv. **5**, eaaw1634 (2019).
[44] A. J. White and L. A. Collins, Phys. Rev. Lett. **125**, 055002 (2020).
[45] A. D. Baczewski, L. Shulenburger, M. P. Desjarlais, S. B. Hansen, and R. J. Magyar, Phys. Rev. Lett. **116**, 115004 (2016).
[46] A. Yilmaz, K. Hunger, T. Dornheim, S. Groth, and M. Bonitz, J. Chem. Phys. **153**, 124114 (2020).
[47] S. D. Baalrud, Phys. Plasmas **19**, 030701 (2012).
[48] S. D. Baalrud and J. Daligault, in *Proceedings of the 30th International Symposium on Rarefied Gas Dynamics (RGD30)*, edited by A. Ketsdever and H. Struchtrup, AIP Conf. Proc. No. 1786 (AIP Publishing, New York, Melville, 2016), p. 130001.
[49] F. Trintchouk, M. Yamada, H. Ji, R. M. Kulsrud, and T. A. Carter, Phys. Plasmas **10**, 319 (2003).
[50] A. Kuritsyn, M. Yamada, S. Gerhardt, H. Ji, R. Kulsrud, and Y. Ren, Phys. Plasmas **13**, 055703 (2006).
[51] M. P. Desjarlais, C. R. Scullard, L. X. Benedict, H. D. Whitley, and R. Redmer, Phys. Rev. E **95**, 033203 (2017).
[52] B. I. Cho, T. Ogitsu, K. Engelhorn, A. A. Correa, Y. Ping, J. W. Lee, L. J. Bae, D. Prendergast, R. W. Falcone, and P. A. Heimann, Sci. Rep. **6**, 18843 (2016).
[53] M. Zaghoo, T. R. Boehly, J. R. Rygg, P. M. Celliers, S. X. Hu, and G. W. Collins, Phys. Rev. Lett. **122**, 085001 (2019).
[54] L. D. Landau and E. M. Lifshitz, *Quantum Mechanics*, Course of Theoretical Physics, Vol. 3 (Pergamon Press, Oxford, 1965).
[55] T. Sakurai and S. F. Tuan, in *Modern Quantum Mechanics*, edited by J. J. Sakurai and S. F. Tuan (Addison-Wesley Pub., Reading, MA, 1994).